UNIVERSITÀ DEGLI STUDI DI PADOVA

FACOLTÀ DI SCIENZE MM.FF.NN.
DIPARTIMENTO DI FISICA "GALILEO GALILEI"

LAUREA TRIENNALE IN FISICA

Bose-Einstein Correlations in proton-proton collisions with the CMS Detector

Relatore: Dott Paolo Ronchese
Correlatore: Dott Paolo Checchia
Laureando: Mattia Francesco Moro

ANNO ACCADEMICO 2009/2010

Chapter 1

Introduction

Particle interferometry constitutes an important method to obtain information about space-time aspects of multiple particle production and, using the Bose-Einstein correlation (BEC), the structure of the hadronization source can be studied. BEC effects are made manifest by the enhanced emission of boson pairs with small relative momenta. The first application of these studies was oriented to astrophysics. Hanbury-Brown and Twiss, in order to measure the stars's diameter, used the correlation of the photons arriving to two telescopes[1]. Only in the fifties, four particle physicist, Goldhaber S., Goldhaber G., Lee and Pais [2] used BEC to gather information about the collision source in a $p\overline{p}$ collision.

1.1 Bose Einstein correlation

Bose Einstein correlation arises as a consequence of quantum statistical interference between the wave functions of particles with integer spin. The effect appears as an increase of the number of the boson pairs detected in the same cell in phase space and the function that describes this correlation is:

$$C_2(p_1, p_2) = \frac{N_{1,2}(p_1, p_2)}{[N_1(p_1) \cdot N_2(p_2)]} \tag{1.1}$$

where $N_{1,2}$ is related to the differential cross section σ measured for a pair of boson with same mass $\left(N_{1,2} = \frac{1}{\sigma}\frac{d^2\sigma}{d\Omega_1 d\Omega_2}\right)$ detected simultaneously whereas N_i is related to the differential cross section detected separately:

$$N_i(p_i) = \frac{1}{\sigma}\frac{d\sigma}{d\Omega_i}, \qquad d\Omega_i = \frac{d^3\vec{p_i}}{(2\pi)^3 2E_{p_i}}, \qquad E_{p_i} = \sqrt{\vec{p_i}^2 + m^2}, \quad i = 1, 2 \tag{1.2}$$

The formula 1.1 can be expressed as

$$R = \frac{P(p_1, p_2)}{P(p_1)P(p_2)} \tag{1.3}$$

where P is the probability function of the four-momenta of the particle. Since Bose-Einstein correlation cannot be measured directly, while it is possible to calculate the correlation of particles, the problems that arise are to build a sample of uncorrelated pairs (that represents the denominator of formula 1.1), preferably from the data, and

choose a probability function. Experimentally R is measured using the distribution of the variable Q:

$$Q = \sqrt{-(p_1 - p_2)^2} = \sqrt{m_{inv}^2 - 4m_\pi^2} \tag{1.4}$$

where m_{inv} is the invariant mass of the two particles, assumed to be pions with mass m_π. The ratio R is obtained by dividing the Q distribution of pairs of same-charge particles by a reference sample built with pairs of particles which by construction are expected to have no Bose-Einstein correlation:

$$R = \frac{dN/dQ}{dN/dQ_{ref}} \tag{1.5}$$

A wide range of possible functions, describing the shape of the BEC, is enumerated in literature; among them we find the Goldhaber-like parametrization whose simplest version is:

$$R(Q) = C[1 + \lambda\Omega(Qr)] \cdot (1 + \delta\ Q) \tag{1.6}$$

where C is the normalization factor, λ is the "chaoticy strenght factor", $\Omega(Qr)$ is the Fourier transform of the emission region, δ accounts for long-distance correlations or biases introduced by the use of non-ideal reference samples [3]. The Fourier transform of the emission region can be modeled in various forms: $\Omega(Qr) = e^{-Qr/\hbar c}$ (exponential); $\Omega(Qr) = e^{-(Qr/\hbar c)^2}$(Gaussian); $\Omega(Qr) = 1/(1 + Qr/\hbar c)^2$; etc.

1.2 CMS experiment

The Large Hadron Collider(CERN), the world's largest and highest-energy particle accelerator, was designed to collide proton beams, up to the center of mass energy of 14 TeV, or lead nuclei. The beams collide in 4 points where four experiments are placed: CMS, ATLAS, ALICE, and LHCb. On 30 March 2010 the first collisions were recorded at 7TeV in the center of mass.
This analysis uses data taken from CMS (Compact Muon Solenoid) [4]; the experiment has a cylindrical structure coaxial to the beam pipe with a diameter of 14.6 m and a length of 21.6 m. The main parts of the experiment are listed in the following; they are ordered with increasing distance from the collision point.

The tracker: It is the detector closest to the interaction point and it is used to reconstruct the tracks of individual particles and the vertices from which they originated; it is composed by two main parts: silicon pixel and the silicon strip detector.

The Electromagnetic Calorimeter (ECAL): It is used to measure the energy of photons and electrons and it is made of more than 70.000 lead tungstate ($PbWO_4$) scintillating crystals.

The Hadronic Calorimeter (HCAL): It is used to measure the energy of hadronic jets and it is composed of layers of dense material (brass or steel) interleaved with tiles of plastic scintillators, read out via wavelength-shifting fibres by hybrid photodiodes.

The magnet: The superconducting magnet for CMS has been designed to reach a 4T field in a cylinder of 6-m diameter and 12.5-m length with a stored energy of 2.6 GJ at full current; the flux is returned through an iron yoke segmented in 5 wheels and 2 endcaps, composed of three disks each.

The muon detectors: They are placed outside the magnets, they are gaseous detectors: drift tube chambers (in the barrel), cathode strip chambers (in the end caps), and resistive plate chambers. This setup is used for precise trajectory measurements and fast trigger.

The position and momenta of particle in the experiment are described in a system of coordinates centered in the center of the experiment itself. Cartesian coordinates are defined taking the x axis pointing towards the center of LHC; the y axis is orthogonal to LHC plane and the z axis is oriented along the beams. Another system of coordinates is also used, due to the cylindrical shape of the experiment. In that system r is the distance from the beams axis, θ is the polar angle and ϕ is the azimuth. In place of the polar angle another variable, pseudorapidity, is used; it's defined as:

$$\eta = -\log\left(\tan\frac{\theta}{2}\right) = \log\left(\frac{p + p_{\parallel}}{p - p_{\parallel}}\right)$$

where p is particle's momentum, $p_{\parallel}$ is p z-component ($p_{\parallel} = p\cos\theta$), p_T is the component transverse to beams direction ($p_T = p\sin\theta$).

Chapter 2

Data description and selection

2.1 Data samples

The data analyzed in this thesis are collected by the CMS experiment in a few days at the beginning of the 2010 proton-proton LHC run at a 7 TeV centre of mass energy. Events were selected requiring activity in the beam scintillator detectors. In addition the event must contain at least 2 and at most 150 charged particles.
Four different simulated samples (D6T, ProPt0, Perugia0 (P0), Pythia8) were analyzed: the former three are produced with Pythia[1] 6, with different tuning, while the latter was produced with Pythia 8. The generated Monte Carlo samples don't include Bose-Einstein simulation; more details are given in section 3.2. A preliminary analysis was done on the real CMS data and on all MC samples, comparing the distribution of N(particles multiplicity), p, p_T, η and charge, before and after the cuts (explained in next section) in order to verify a consistence between real and simulated data.

2.2 Track Selection

In order to correctly analyze the data, several cuts are needed: some of them due to the type of particles that we analyze (low-momentum pions) and others due to the limitations of the detector.
The particles have to pass from the primary vertex through three silicon pixel detectors so only those with $p_T > 200$ MeV/c are accepted. Due to the tracker acceptance the particle pseudorapidity (η_{track}) is required to be less then 2.4. To ensure high purity of the primary track selection, particles are required to be reconstructed by fits with more than five degrees of freedom and $\chi^2/N_{dof} < 5.0$.
The particle samples contains electrons, positrons from photon conversions in the detector material and secondary particles from the decay of long-lived hadrons (K^0_S, Λ, etc.). They are removed requiring the transverse impact parameter with respect to the collision point to be $|d_{xy}| < 0.15$ cm, and the innermost measured point of the track to have a radius $r < 20$ cm.
Ghosts tracks are produced when hits from single track are splitted in two by the pattern recognition alghoritm. These ghost tracks are removed by a further selection if $|\vec{p}_{T_i} - \vec{p}_{T_j}| < 40 MeV/c$, and $\cos\theta_{i,j} > 0.99996$ (θ is the angle between tracks i, j)[5].

[1] Pythia is an event generator for a large number of physics processes

A total of 2,701,945 events are selected at 7 TeV center-of-mass energy and 94,513,656 tracks are accepted by the above selection criteria.

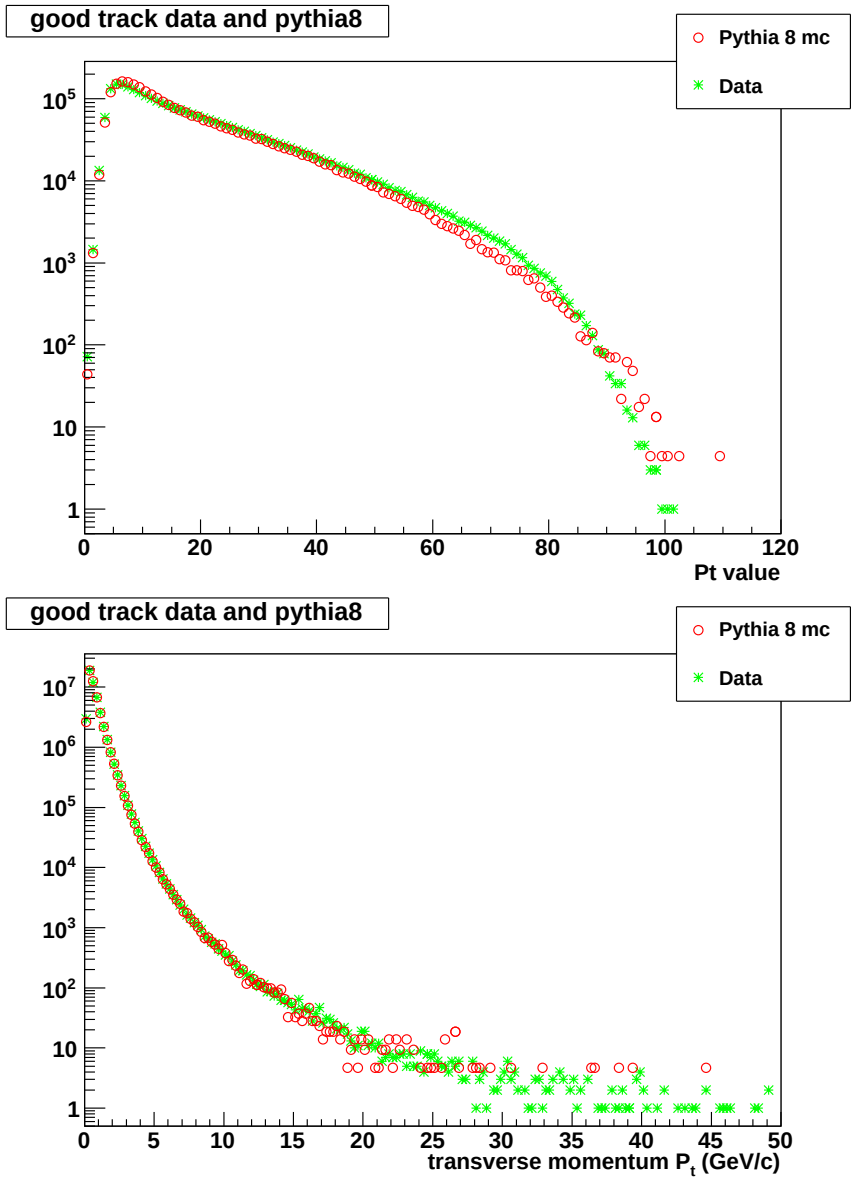

Figure 2.1: Distribution of Track Multiplicity and p_T after cuts for real data and Pythia 8 Tune

Chapter 3

Definition of signal and reference sample

3.1 Signal

The signal is observed in the distribution of the Q-value for pairs of same charge tracks belonging to the same event. The interval considered is limited between 0.02 and 2 GeV: the lower limit is imposed in order to remove possible tracks reconstructed incorrectly [1] while the upper limit allows for a wide-enough side band for the normalization of the reference sample.

3.2 Reference Sample

In order to find a sample of particle pairs that does not present BEC, and could be used in the formula 1.5, several reference samples were produced that a priori shouldn't show this effect. The sample produced are:

Opposite-charge pairs: this sample may seem a priori the best reference but it contains pairs of particle coming from low mass resonances (η, ρ), not present in the signal. This requires to remove the Q-range between 0.6 and 0.9 GeV, (Figure 3.1a);

Opposite-hemisphere pairs: particle pairs are constructed after inverting in space the three-momentum of one of the two particles: $(\mathrm{E}, \overrightarrow{p}) \rightarrow (\mathrm{E}, -\overrightarrow{p})$. This procedure is applied to pairs with same and opposite charges.(Figure 3.1b,3.1c);

Rotated particles: a statistically-independent reference sample is constructed by inverting the x, y components of the three-momentum of one of the two particles and leaving the z component of momentum unchanged: $(p_x, p_y, p_z) \rightarrow (-p_x, -p_y, p_z)$.(Figure 3.1d);

While the previous samples were built by combining tracks in the same event the following are made by combining tracks in different events.

Random order: events are paired at random (Figure 3.1e);

[1] the track recognition algorithm fails and produces two tracks for one particle or one track for two particles

Same η: events with similar charged particles density in the same η regions are selected ($-2.4 < \eta < -0.8, |\eta| < 0.8, 0.8 < \eta < 2.4$) (Figure 3.1f);

Same Mass: events with an invariant mass ($M = \sum_i p_i^2$) of all charged particles similar to that of the signal are paired. (Figure 3.1g);

The following methods were also tried (using tracks from different events); they produced results similar to the ones obtained with previous samples so they were not used for final results.

Same Sphericity: events with similar sphericity [2];

Same Sphericity, Rotated: events with similar sphericity and rotated in order to have same sphericity axes [3];

Same Multiplicity, η Binned: event with same number of track, with similar charged particle density in 10 (η) regions ($-3< \eta\leq-2.4$, $-2.4<\eta\leq-1.8$, $-1.8<\eta\leq-1.2$, $-1.2<\eta\leq-0.6$, $-0.6<\eta\leq0$ and the symmetric regions in range 0-3);

Same Multiplicity, η Binned and Rotated: events with same number of tracks, with similar charged particle density in 10 (η) regions and rotated by sphericity axis.

[2]Sphericity is defined as the squared summed transverse moment with respect to the event axis [6].The sphericity tensor is:

$$S^{\alpha\beta} = \frac{\sum_i p_i^\alpha p_i^\beta}{\sum_i |p_i|} \tag{3.1}$$

where α, β = 1,2,3 corrispond to the x, y and z components of every track's momentum vector. From the normalized eigenvalues of sphericity tensor (λ_2, λ_3) we can calculate sphericity $S = \frac{3}{2}(\lambda_2 + \lambda_3)$.

[3]Sphericity axis are the three normalized eigenvectors of sphericity Tensor 3.1

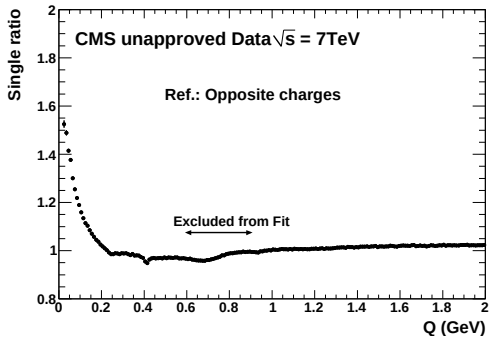

(a) Opposite charge

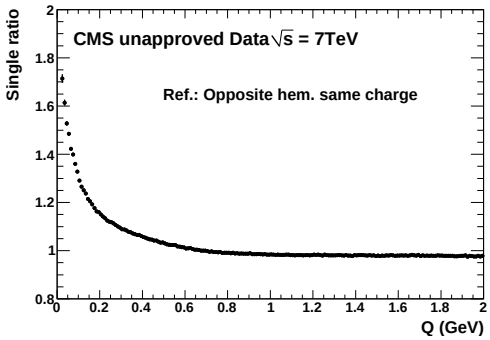

(b) Opposite hemisfere same charge

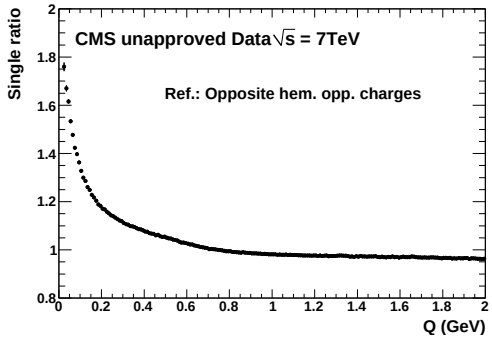

(c) Opposite hemisfere diff. charge

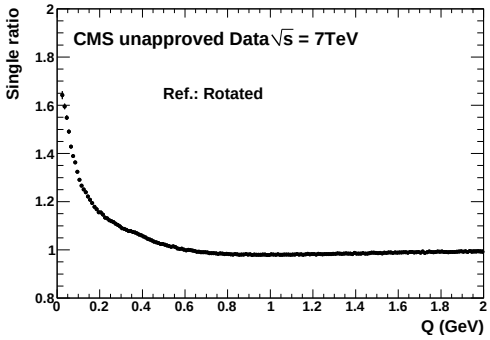

(d) Rotated

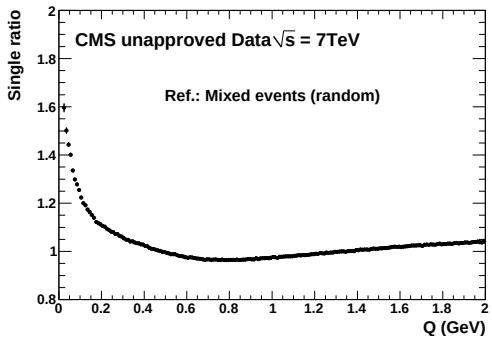

(e) Random Mixing

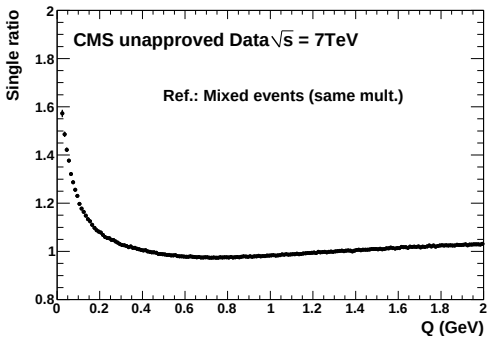

(f) η Mixing

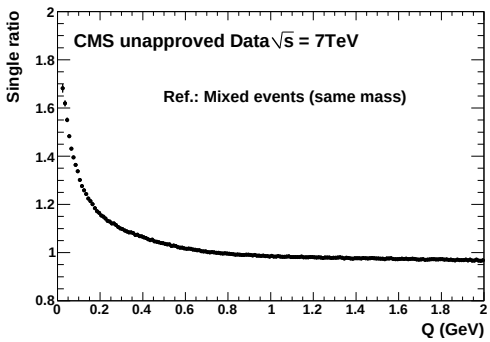

(g) Mass Mixing

Figure 3.1: Distribution of the ratio R (eq 1.5), for the 7 TeV data

Chapter 4

Determination of Bose-Einstein Correlation Parameters

As seen in section 1.1 there are several functions that can describe the BEC. In this analysis the exponential form has been chosen for $\Omega(Qr)$ (cfr. eq. 1.6), so the function describing the ratio R is:

$$R(Q) = C[1 + \lambda e^{-Qr/\hbar c}] \cdot (1 + \delta\ Q) \tag{4.1}$$

The reference samples listed in section 3.2 were constructed directly from the data and they were used to build ratio R (cfr. eq. 1.5).

4.1 Coulomb corrections

The Coulomb interaction changes the relative momentum distribution between pairs of particles considered. It is therefore necessary to apply the correction factors (called Gamow factors [7]) expressed by the following equations:

$$W_s(\eta) = \frac{e^{2\pi\eta} - 1}{2\pi\eta} \qquad W_d(\eta) = \frac{1 - e^{-2\pi\eta}}{2\pi\eta} \tag{4.2}$$

with $\eta = \alpha_{em} m_\pi / Q$ where $\alpha_{em} = \frac{1}{137}$ is the electromagnetic constant. This type of correction is not applied to samples produced by Monte Carlo as the Coulomb interaction is not simulated; same charge sample (signal) and opposite charge sample, extracted from the real data, need to be corrected with W_s and W_d respectively.

4.2 Single Ratio

The results obtained from a fit to $R(Q)$ with eq 4.1 are shown in table 4.1. It is evident that they are quite scattered and no reference can be considered satisfactory enough: as we can se in figures 3.1 none of them has a constant value in range 0.8-1, and all $\frac{\chi^2}{NDOF}$ in table 4.1 have values grater than 10.

Label	$\frac{\chi^2}{NDOF}$	C	λ	r(fm)	δ
Ref.: Opposite charges	24.7	0.96 ± 0.01	0.89 ± 0.01	2.72 ± 0.02	$4.14 \cdot 10^{-2} \pm \cdot 10^{-4}$
Ref.: Opposite hem. same charge	13.5	0.99 ± 0.01	0.52 ± 0.01	1.00 ± 0.02	$-5.53 \cdot 10^{-3} \pm 3.92 \cdot 10^{-4}$
Ref.: Opposite hem. opp. charges	23.0	0.99 ± 0.01	0.50 ± 0.01	0.85 ± 0.02	$-1.44 \cdot 10^{-2} \pm 4.57 \cdot 10^{-4}$
Ref.: Rotated	12.7	0.96 ± 0.01	0.57 ± 0.01	0.92 ± 0.01	$2.13 \cdot 10^{-2} \pm 4.47 \cdot 10^{-4}$
Ref.: Mixed events (random)	14.1	0.89 ± 0.01	0.58 ± 0.01	0.85 ± 0.02	$9.21 \cdot 10^{-2} \pm 6.51 \cdot 10^{-4}$
Ref.: Mixed events (same mult.)	11.3	0.93 ± 0.01	0.53 ± 0.01	1.19 ± 0.02	$5.34 \cdot 10^{-2} \pm 3.81 \cdot 10^{-4}$
Ref.: Mixed events (same mass)	13.1	1.00 ± 0.01	0.50 ± 0.01	1.02 ± 0.02	$-1.80 \cdot 10^{-2} \pm 3.73 \cdot 10^{-4}$

Table 4.1: Fit results for ratio R in data

4.3 Double Ratio and different Monte Carlo tunes

To reduce the sensibility of our results to the choice of the reference sample, the following quantity was built:

$$\mathcal{R} = \frac{R}{R_{MC}} = \left(\frac{dN/dQ}{dN/dQ_{ref}} \right) / \left(\frac{dN/dQ_{MC}}{dN/dQ_{MC,ref}} \right) \tag{4.3}$$

where"MC" and "MC,ref" refer to the respective distributions produced from the simulated data. In the following this ratio $\mathcal{R}$ will be named "double ratio" opposed to the "single ratio" R computed only in data. In each fit the reference samples for data and simulation are obtained in the same way. As mentioned in the introduction several Monte Carlo samples are used and the same analysis was repeated for each of them.

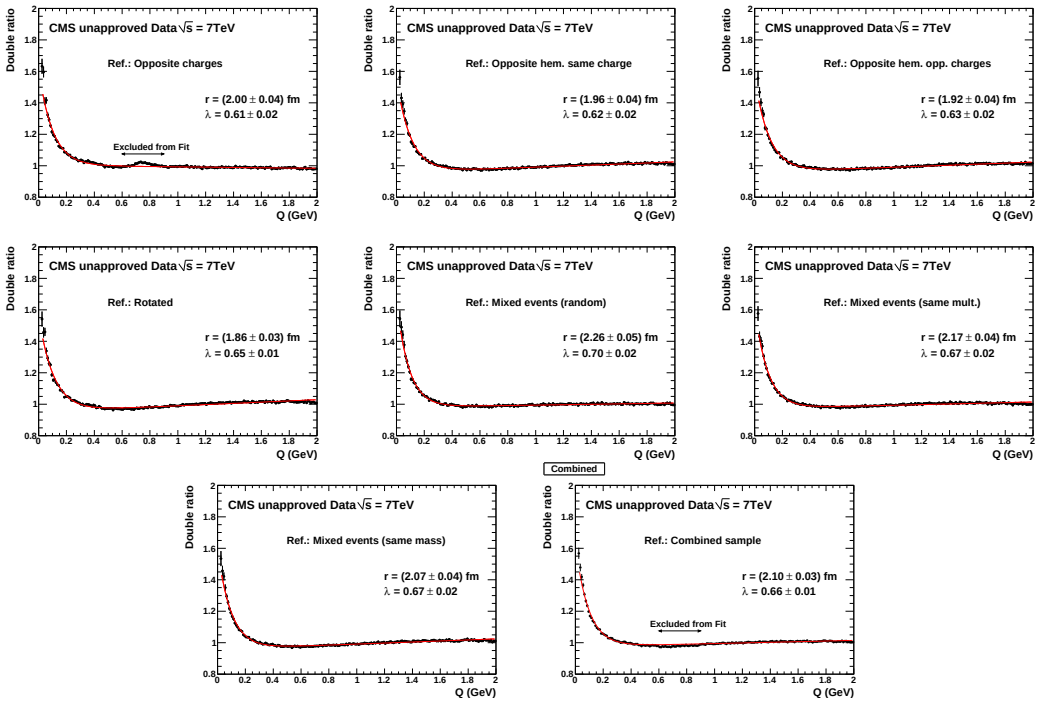

Figure 4.1: Distribution of the double ratio $\mathcal{R}$, for the 7 TeV data for P0 MC tune.

As can be seen in table 4.2 only Perugia0, ProPt0 and Pythia8 samples produce distributions properly described by the correlation function; on the other hand, the

Perugia 0

Label	$\frac{\chi^2}{NDOF}$	C	λ	r(fm)	$\delta(GeV^{-1})$
Ref.: Opposite charges	3.59	1.01 ± 0.01	0.64 ± 0.01	2.04 ± 0.03	$-9.26 \cdot 10^{-3} \pm 4.67 \cdot 10^{-4}$
Ref.: Opposite hem. same charge	3.31	0.96 ± 0.01	0.64 ± 0.01	1.95 ± 0.02	$3.57 \cdot 10^{-2} \pm 4.47 \cdot 10^{-4}$
Ref.: Opposite hem. opp. charges	3.31	0.96 ± 0.01	0.64 ± 0.01	1.91 ± 0.02	$3.50 \cdot 10^{-2} \pm 4.50 \cdot 10^{-4}$
Ref.: Rotated	7.73	0.95 ± 0.01	0.66 ± 0.01	1.86 ± 0.02	$4.12 \cdot 10^{-2} \pm 4.55 \cdot 10^{-4}$
Ref.: Mixed events (random)	2.04	0.98 ± 0.01	0.70 ± 0.01	2.25 ± 0.03	$1.33 \cdot 10^{-2} \pm 4.46 \cdot 10^{-4}$
Ref.: Mixed events (same mult.)	4.94	0.97 ± 0.01	0.67 ± 0.01	2.14 ± 0.02	$2.19 \cdot 10^{-2} \pm 4.06 \cdot 10^{-4}$
Ref.: Mixed events (same mass)	3.47	0.96 ± 0.01	0.67 ± 0.01	2.08 ± 0.02	$3.55 \cdot 10^{-2} \pm 4.33 \cdot 10^{-4}$
Avg. Ref. Sample	4.64	0.97 ± 0.01	0.67 ± 0.01	2.10 ± 0.02	$2.14 \cdot 10^{-2} \pm 3.74 \cdot 10^{-4}$

ProPT0

Label	$\frac{\chi^2}{NDOF}$	C	λ	r(fm)	$\delta(GeV^{-1})$
Ref.: Opposite charges	2.00	1.00 ± 0.01	0.60 ± 0.02	1.88 ± 0.04	$-1.02 \cdot 10^{-2} \pm 7.45 \cdot 10^{-4}$
Ref.: Opposite hem. same charge	1.76	0.98 ± 0.01	0.61 ± 0.01	1.83 ± 0.03	$1.56 \cdot 10^{-2} \pm 6.70 \cdot 10^{-4}$
Ref.: Opposite hem. opp. charges	1.83	0.98 ± 0.01	0.62 ± 0.02	1.84 ± 0.03	$1.32 \cdot 10^{-2} \pm 6.69 \cdot 10^{-4}$
Ref.: Rotated	2.98	0.96 ± 0.01	0.62 ± 0.01	1.67 ± 0.03	$2.81 \cdot 10^{-2} \pm 7.15 \cdot 10^{-4}$
Ref.: Mixed events (random)	1.55	1.01 ± 0.01	0.70 ± 0.02	2.32 ± 0.05	$-1.59 \cdot 10^{-2} \pm 6.24 \cdot 10^{-4}$
Ref.: Mixed events (same mult.)	2.19	0.98 ± 0.01	0.63 ± 0.02	1.98 ± 0.04	$1.90 \cdot 10^{-2} \pm 6.35 \cdot 10^{-4}$
Ref.: Mixed events (same mass)	1.93	0.97 ± 0.01	0.63 ± 0.02	1.92 ± 0.03	$1.75 \cdot 10^{-2} \pm 6.51 \cdot 10^{-4}$
Avg. Ref. Sample	2.11	0.99 ± 0.01	0.64 ± 0.01	1.99 ± 0.03	$7.12 \cdot 10^{-3} \pm 5.73 \cdot 10^{-4}$

Pythia 8

Label	$\frac{\chi^2}{NDOF}$	C	λ	r(fm)	$\delta(GeV^{-1})$
Ref.: Opposite charges	7.05	1.00 ± 0.01	0.65 ± 0.01	2.17 ± 0.03	$-4.76 \cdot 10^{-3} \pm 4.20 \cdot 10^{-4}$
Ref.: Opposite hem. same charge	3.60	0.98 ± 0.01	0.56 ± 0.01	1.60 ± 0.02	$1.07 \cdot 10^{-2} \pm 4.38 \cdot 10^{-4}$
Ref.: Opposite hem. opp. charges	4.26	0.98 ± 0.01	0.56 ± 0.01	1.52 ± 0.02	$9.37 \cdot 10^{-3} \pm 4.52 \cdot 10^{-4}$
Ref.: Rotated	5.98	0.96 ± 0.01	0.58 ± 0.01	1.43 ± 0.01	$2.65 \cdot 10^{-2} \pm 4.76 \cdot 10^{-4}$
Ref.: Mixed events (random)	2.91	1.00 ± 0.01	0.64 ± 0.01	1.92 ± 0.02	$-9.43 \cdot 10^{-3} \pm 4.16 \cdot 10^{-4}$
Ref.: Mixed events (same mult.)	4.18	0.98 ± 0.01	0.59 ± 0.01	1.74 ± 0.02	$1.43 \cdot 10^{-2} \pm 4.09 \cdot 10^{-4}$
Ref.: Mixed events (same mass)	3.49	0.98 ± 0.01	0.60 ± 0.01	1.67 ± 0.02	$1.40 \cdot 10^{-2} \pm 4.25 \cdot 10^{-4}$
Avg. Ref. Sample	4.97	0.99 ± 0.01	0.61 ± 0.01	1.80 ± 0.02	$5.19 \cdot 10^{-3} \pm 3.71 \cdot 10^{-4}$

D6T

Label	$\frac{\chi^2}{NDOF}$	C	λ	r(fm)	$\delta(GeV^{-1})$
Ref.: Opposite charges	5.17	1.01 ± 0.01	0.47 ± 0.01	1.40 ± 0.02	$-1.63 \cdot 10^{-2} \pm 6.18 \cdot 10^{-4}$
Ref.: Opposite hem. same charge	7.39	0.97 ± 0.01	0.73 ± 0.01	2.45 ± 0.03	$2.54 \cdot 10^{-2} \pm 4.20 \cdot 10^{-4}$
Ref.: Opposite hem. opp. charges	6.69	0.97 ± 0.01	0.73 ± 0.01	2.47 ± 0.03	$2.41 \cdot 10^{-2} \pm 4.15 \cdot 10^{-4}$
Ref.: Rotated	10.0	0.93 ± 0.01	0.70 ± 0.01	2.09 ± 0.02	$5.46 \cdot 10^{-2} \pm 4.71 \cdot 10^{-4}$
Ref.: Mixed events (random)	46.6	0.62 ± 0.01	0.64 ± 0.02	-0.13 ± 0.01	$-0.28 \pm 1.5 \cdot 10^{-2}$
Ref.: Mixed events (same mult.)	49.0	0.81 ± 0.01	0.26 ± 0.01	-0.24 ± 0.01	$-0.35 \pm 1.2 \cdot 10^{-2}$
Ref.: Mixed events (same mass)	47.2	0.79 ± 0.01	0.27 ± 0.01	-0.24 ± 0.01	$-0.35 \pm 1.2 \cdot 10^{-2}$
Avg. Ref. Sample	11.3	0.98 ± 0.01	0.75 ± 0.01	2.55 ± 0.03	$1.35 \cdot 10^{-2} \pm 3.48 \cdot 10^{-4}$

Table 4.2: Double Ratio's fit results for every Monte Carlo at 7 TeV. The last line of each set of fits shows the result obtained by combining the reference samples as described in Section 4.4. Errors are statistical only, and quoted as if independent.

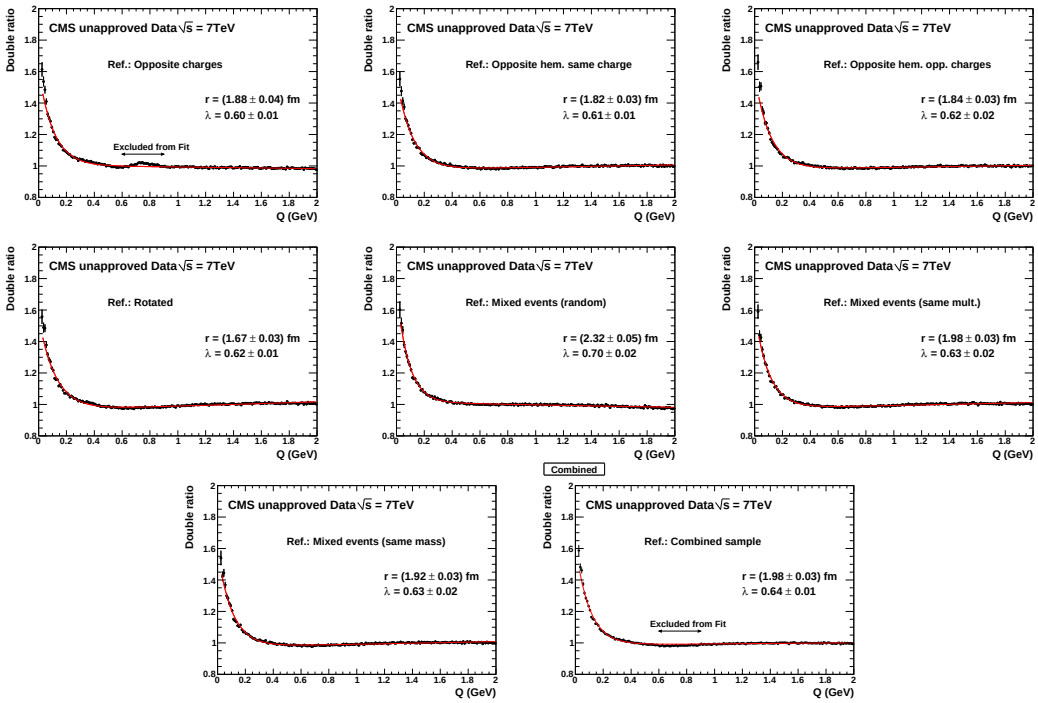

Figure 4.2: Distribution of the double ratio $\mathcal{R}$, for the 7 TeV data for ProPt0 MC tune.

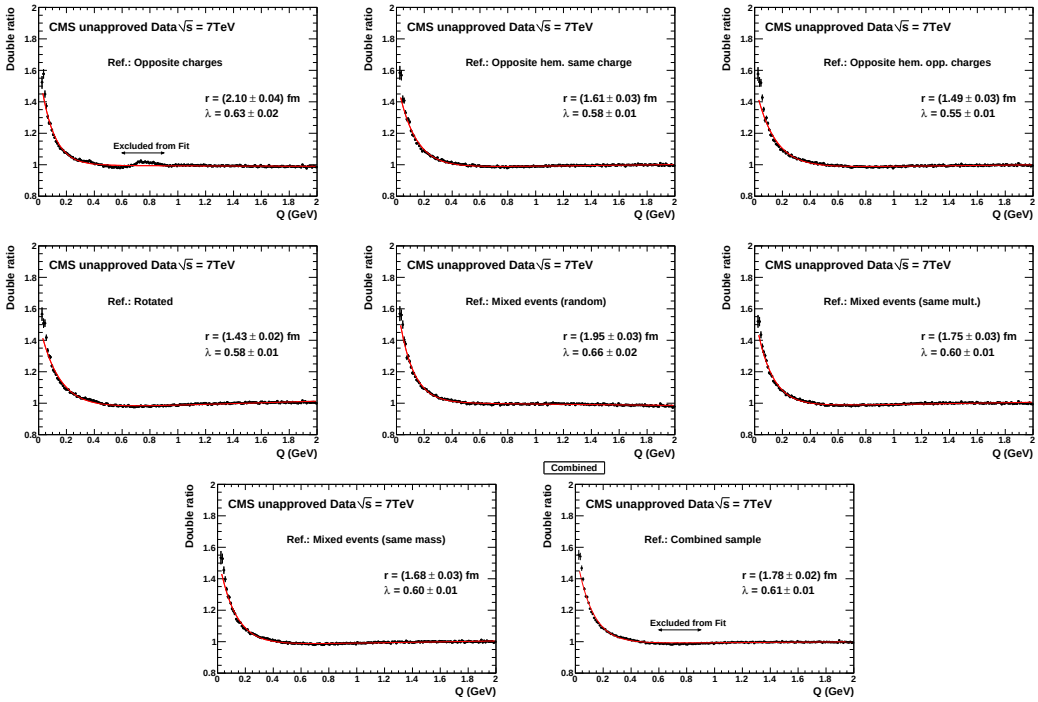

Figure 4.3: Distribution of the double ratio $\mathcal{R}$, for the 7 TeV data for Pythia8 MC tune.

D6T doesn't fit properly for all reference samples.
In addition it must be noticed that an effect is present, not considered so far: for all the Monte Carlo samples double ratio in the range 0.4-1 GeV shows a dip as shown in figure 4.4. The dip constitutes a few percent effect; it is present in all MC datasets with some variation in its depth, but it is sufficient to spoil the fit quality of the used function. Regarding the D6T in the range 1.4-2 GeV the $\mathcal{R}$ distribution goes down, while for the others (Perugia0, ProtPt0, Pythia8), it remain almost constant. This behavior is not reproduced by the selected function so D6T has been discarded.

4.4 Combined sample and all reference combined sample

The experimental technique of taking a double ratio between data and Monte Carlo ratios of the Q-value distributions, to determine the parameters of the BEC effect, reduces considerably the sources of bias due to track inefficiency and other detector-related effects. Still, a sizeable spread can be observed in the measurements obtained with different reference samples. As any of these samples can introduce not easily-predictable biases, none of them is a-priori preferable. In order to provide a single value for each of the fit parameters together with an estimate of the systematic error connected for each Monte Carlo (only Perugia0, ProPt0, Pythia8 are now considered), the double ratio $\mathcal{R}$ was computed by using the following formula:

$$\mathcal{R}^{avg} = \frac{dN/dQ}{dN/dQ_{MC}} \left(\frac{\sum_{s=1}^{N_S} dN/dQ_{MC,s}}{\sum_{s=1}^{N_S} dN/dQ_s} \right) \tag{4.4}$$

Where s labels the reference (as described in par 3.2) and ranges from 1 to $N_S = 7$. This approach is motivated by these considerations:

- it deals paritetically with the abundance of used reference samples;
- it accounts properly (and easily) for the statistical correlations between the different measurements, all sharing the same signal, but differing for the composition of the reference sample;
- it allows an easy and well-defined estimate of the systematic uncertainty related to the choice of the reference sample.

In order to obtain a global result for this analysis an all-combined reference is constructed using the three selected Monte Carlo (Perugia0, ProPt0, Pythia8):

$$\mathcal{R}^{combined\ avg} = \frac{dN/dQ}{\sum_{mc=1}^{N_{MC}} dN/dQ_{mc}} \sum_{s=1}^{N_s} \frac{\sum_{mc=1}^{N_{MC}} dN/dQ_{mc,s}}{dN/dQ_s} \tag{4.5}$$

where s labels the reference as before, mc labels the Monte Carlo samples and ranges from 1 to $N_{MC} = 3$. The result is shown in figure 4.5 and in table 4.3

C	λ	r(fm)	$\delta(GeV^{-1})$
0.98 ± 0.01	0.64 ± 0.01	1.95 ± 0.02	$1.03 \cdot 10^{-4} \pm 3.87 \cdot 10^{-4}$

Table 4.3: Fit results for all combined sample

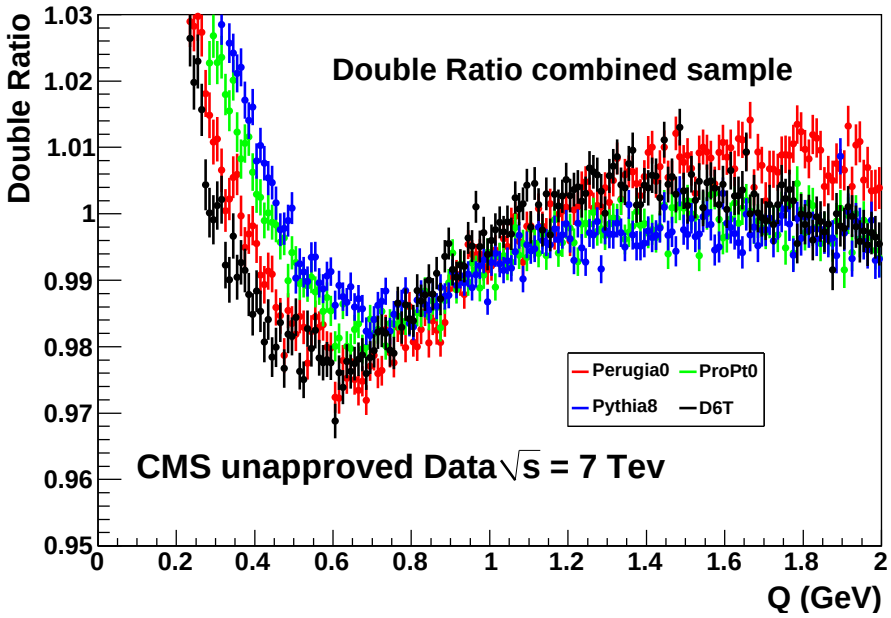

Figure 4.4: Different Monte Carlo behavior for combined samples

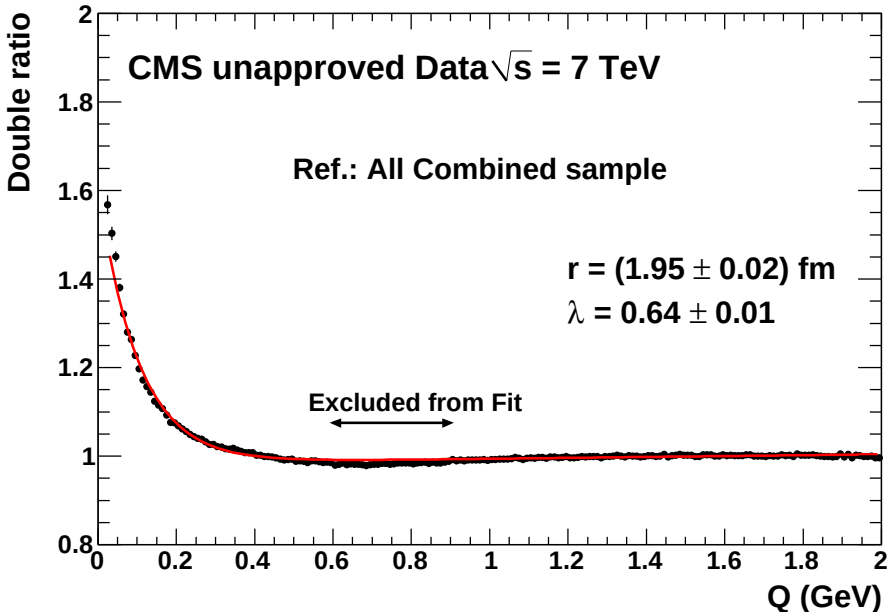

Figure 4.5: Combined reference using Perugia0, ProPt0, Pythia8

4.5 Systematic Uncertainties

A systematic uncertainty on the measurements arises from the fact that none of the reference samples is expected to give a perfect description of the Q distribution in the absence of BEC, and none of them can be preferred or discarded a priori. The systematic uncertainty is thus computed as the r.m.s. spread between the results obtained using the different reference samples, i.e. $\pm 4\%$ for λ and $\pm$ 11% for r. The uncertainty related to the Coulomb corrections was determined with the opposite-charge sample, the predicted strength of the Coulomb effect being compatible with the data within $\pm$ 15%. The corresponding changes are 0.8% for r and 2.8% for λ, which are used as systematic errors. In addition to the main systematic due to the choice of the reference sample, it is clear that the fitted 7 TeV BEC parameters depend on the MC tune. To evaluate the error contribution due to the MC dataset the r.m.s. spread of the results obtained with the All-combined-MC productions has been taken, i.e. $\pm 5\%$ for λ and $\pm$ 8% for r. All the contributions to the systematic error are reported in table 4.4.

Source	λ	r
Choice of the reference sample	0.029	0.179
All-combined MC reference	0.030	0.151
Effect of Coulomb corrections	0.018	0.016
Total	0.045	0.234

Table 4.4: Summary of the systematic uncertainties

The total systematic uncertainty is given as the quadratic sum of the single contribution.

Chapter 5

Conclusions

Bose-Einstein correlations have been measured using data collected by the CMS experiment at the LHC from *pp* collisions at 7 TeV centre-of-mass energy. Several reference samples and Monte Carlo were used to extract the results.
Two aspects must be taken into account:

- The presence of a dip in the double ratio shown in figure 4.4 from 0.3 and 1 GeV (it is also present in hadronic Z^0 decays in LEP [8]).
- The fit function doesn't consider all the range in the combined sample (the range 0.6-1.0 GeV). This is due to the presence of resonances in the opposite charge sample (as explained in §3.2).

In order to obtain a global result an all-combined sample was built and the BEC parameters extracted from fits using an exponential form results are: $r = 1.95 \pm 0.02$ (stat.) $\pm$ 0.23 (syst.) fm and $\lambda = 0.64 \pm 0.01$ (stat.) $\pm$ 0.05 (syst.) at 7 TeV. This is the first measurement of Bose-Einstein Correlations at 7 TeV *pp* collisions and the result is compatible within the errors with the one obtained by CMS at 900 GeV.

Bibliography

[1] Hanbury-Brown R. and Twiss R. Q. . A new type of interferometer for use in radio astronomy. *Philosophical Magazine*, 45(366):663–682, 1954.

[2] Goldhaber, Gerson and Fowler, William B. and Goldhaber, Sulamith and Hoang, T. F. and Kalogeropoulos, Theodore E. and Powell, Wilson M. Pion-Pion Correlations in Antiproton Annihilation Events. *Phys. Rev. Lett.*, 3(4):181–183, 1959.

[3] Kozlov, G A. Bose-Einstein correlations of neutral gauge bosons in *pp* collisions. Technical Report arXiv:0801.2340, Jan 2008.

[4] CMS Collaboration. The CMS experiment at the CERN LHC. *JINST*, 3(08):S08004, 2008.

[5] CMS Collaboration. First Measurement of Bose-Einstein Correlations in proton-proton Collisions at $\sqrt{s}$ = 0.9 and 2.36 TeV at the LHC. *Phys. Rev. Lett.*, 105:032001, 2010.

[6] T. Sjostrand, S. Mrenna, and P. Skands. Pythia 6.4 physics and manual. *JHEP*, 05:026, 2006.

[7] M. Gyulassy, S. Kaufmann, and L. W. Wilson. Pion interferometry of nuclear collisions. *Phys. Rev. C*, 20:2267, 1979.

[8] W. J. Metzger and T. Novak and W. Kittel and T. Csörgö. Detailed L3 measurements of Bose-Einstein correlations and a region of anti-correlations in hadronic Z^0 decays at LEP. arXiv:1002.1303v1, 2010.